

We are IntechOpen, the world's leading publisher of Open Access books Built by scientists, for scientists

6,900

Open access books available

185,000

International authors and editors

200M

Downloads

Our authors are among the

154

Countries delivered to

TOP 1%

most cited scientists

12.2%

Contributors from top 500 universities



WEB OF SCIENCE™

Selection of our books indexed in the Book Citation Index
in Web of Science™ Core Collection (BKCI)

Interested in publishing with us?
Contact book.department@intechopen.com

Numbers displayed above are based on latest data collected.
For more information visit www.intechopen.com



The Interaction of Tungsten Dust with Human Skin Cells

*Lavinia Gabriela Carpen, Tomy Acsente,
Maria Adriana Acasandrei, Elena Matei,
Claudia Gabriela Chilom, Diana Iulia Savu
and Gheorghe Dinescu*

Abstract

In this chapter, we evaluate the tungsten (W) nanoparticle toxicity with respect to the normal human skin fibroblast cell. Tungsten dust formation is expected in the tokamak-type nuclear fusion installations, regarded as future devices for large-scale, sustainable, and carbon-free energy. This dust, composed of tungsten particles of variable size, from nanometers to micrometers, could be harmful to humans in the case of loss of vacuum accident (LOVA). In order to undertake the toxicity studies, tokamak-relevant dust has been deliberately produced in laboratory and afterward analyzed. Following that, cytotoxicity tests were performed using normal human skin fibroblast cell lines, BJ ATCC CRL 2522. Our study concludes that, at a low concentration (until 100 $\mu\text{g/mL}$), no cytotoxic effect of tungsten nanoparticles was observed. In contrast, at higher concentrations (up to 2 mg/mL), nanometric dust presents toxic effects on the cells.

Keywords: toxicity, tungsten nanoparticles, plasma technology, magnetron sputtering, fusion technology

1. Introduction

Over the past decade, nanotechnology has received a lot of attention, due to its diversity of applications, ranging from electronics, aerospace, computers to biology and nanomedicine. All aspects of our lives have slowly begun to rely on this nanotechnology revolution. Nanotechnology includes the study and manipulation of nanoscale particles. Therefore, this revolution requires the large-scale production of these nanostructures [1]. Due to much smaller dimensions, this nanomaterial presents specific properties, sometimes in contrast with the bulk materials. Beside useful characteristics such as higher values of specific surface/volume ratio, enhanced chemical reactivity, mechanical or physicochemical properties as well as distinct optical properties relative to scale-up materials, these nanomaterials can present a danger to human health. The growing popularity of nanotechnology in medicine has been limited because of the potential side effects caused by the possible toxicity of the nanoparticles [2]. Adverse health effects can be caused by inhalation, oral ingestion, and absorption through the skin or by injection [3]. The studies indicated that the nanoparticle toxicity is observed through cellular modifications

that include cell membrane damage, mitochondrial function affection, apoptosis activation, and also through increased oxidative mechanism stress [4]. These issues have underpinned the development of a new branch of research, under the name of nanotoxicology. Nanotoxicology includes the life cycle study of nanoparticles, in order to better understand the health risks involved in their use. Specific properties, such as particle size, nanoparticle shape, and surface/volume ratio, are considered important factors that directly contribute to nanomaterial toxicity. For example, carbon nanofibers, single-wall nanotubes, and multiwall nanotubes have shown that the toxicity of carbon material depends exclusively on the particles' shape and size [5]. In vivo experiments showed that carbon nanotubes cause granulomatous lung lesions [6] and can also induce platelet aggregation that highlighted a very toxic effect of carbon nanoparticles on the human body.

An element of major importance but not sufficiently introduced in in vitro toxicity evaluation is related to one of the largest organs of the body, the skin. Skin is the barrier between the internal organisms and the external environment. The skin is composed of multilayers and presents on the surface sweat pores, sebaceous glands, and hair sites necessary for hair growth [7]. This is the reason why this large exposure area (18,000 cm²) serves as one of the main inlet ports of nanomaterials inside the body. The tendency of nanomaterials to pass through the skin, thus referring to the mechanism of skin absorption or penetration, is a major factor in the nanomaterial dermatotoxic potential in general, and tungsten (W) nanomaterials especially, mainly taking into account the purpose of this work. The dermatotoxicity produced by nanoparticles was reported primarily by the in vitro experiments. Bennat and Goymann [2, 8] have shown that nanoparticles can penetrate the surface of the skin much more easily by entering through the pores or hair follicles. In general, skin exposure to nanoparticles is mediated through the nanomaterials which are contained in cosmetics or wound dressings. For example, it has been found that sunscreens containing TiO₂ have seeped into the deep parts of the epidermis through the hair sites. Moreover, it's a known fact that silver nanoparticles are effective in treating patients with burns. For example, in the case of Acticoat, a dressing that is coated with silver nanoparticles that is often used for this purpose, there have been various studies that have reported the safety of this drug. Despite this, the toxicity of silver nanoparticles has been reported by a patient with burns of over 30% of the body surface, when they were treated with this silver-coated dressing [2, 9]. Subsequently, dermatotoxicity produced by nanoparticles was also reported in in vivo experiments. Using an animal model study, beryllium particles as large as 0.5 and 1.0 µm in diameter have been shown to be able to penetrate even the epidermis [10], producing toxicity increase on an animal skin.

1.1 Toxicology studies devoted to tungsten at micro- and nanoscale

A nanomaterial with various and multiple applications in the industry, which are rapidly starting to be investigated from a cytotoxicity point of view, is represented by metal nanoparticles. These nanoparticles are widely used in industry and biotechnology, and they are also of great importance in military applications [4]. Thus, the fact that these nanomaterials present potential harmful effects must be urgently researched, especially because they are to be used increasingly [11].

A particular case of metal material is represented by tungsten, a metal with exceptional physical and chemical characteristics. This hard-steel-gray metal is characterized by the highest melting point out of all the discovered elements, highest boiling point, density comparable with uranium or gold, and also low sputtering grade. These properties represent important criteria for which this material is selected as a basic for wall construction in the case of future fusion

devices, like International Thermonuclear Experimental Reactor (ITER). In this case, the expected power and temperature of fusion plasma that directly interact with the tungsten components can trigger the wall erosion and formation of dust in the plasma chamber. This dust, composed of tungsten particles of nanometric and micrometric size, can present safety issues in case of failure of confinement during a loss of vacuum accident (LOVA). Accidental interaction of tungsten nanoparticles can be harmful to fusion device workers [12]. In addition, it is known that metallic nano- and microparticles, when dispersed in the ambient air over certain concentrations, are dangerous for health. The concentration of tungsten particles is reported to be small, less than 10 ng/m^3 in normal situation, in ambient air. But, in industrial processes involving the tungsten production, this concentration is alarming and can reach 62.3 mg/m^3 . Considering this increased concentration, the risk of inhalation or contamination with these nanoparticles is high. Increased tungsten use could lead to contamination of air, water, and soil near tungsten mines or industrial sites [13]. In speciality studies, exposure of W particles has been shown to have no adverse effect at a concentration of up to $100 \text{ }\mu\text{g/mL}$, and the toxic effect is significant at a concentration of at least $250 \text{ }\mu\text{g/mL}$ [1]. For this study, the toxicity was evaluated on liver cells. This cell line is relevant for the toxicity evaluation, because, by ingestion, cells may be exposed to these tungsten particles. However, particles with a diameter of $27 \text{ }\mu\text{m}$ were used. Bolt et al. [14] has shown that tungsten increases breast cancer metastasis as a result of its use in medical devices. Thus, studies that present the toxicity of pure tungsten are mostly focused on its elemental presence or microscale particles, while the reports on this material toxicity at nanoscale size are marginal and extremely rare.

1.2 Toxicology studies devoted to tungsten compounds

Considering the hardness of tungsten carbide, this material is of the greatest interest in the industrial field. In order to develop nanoparticles at a large scale in this area, the potential risks on human health and on the environment have begun to be taken into account. The toxicity of tungsten (WC) and tungsten carbide (WC-Co) doped with cobalt nanoparticles was evaluated on a wide range of mammalian cells (lung, skin, and colon cell lines, as well as in neuronal and glial cells). The WC and WC-Co particles in this study have an average particle size of 145 nm . For the toxicity evaluation, the maximum concentration selected for nanoparticle suspensions was $30 \text{ }\mu\text{g/mL}$. WC nanoparticles have no increased toxicity for these cell lines. However, cytotoxicity became major when the particles were doped with Co. The most sensitive to particles were astrocytes and colon epithelial cells. The findings demonstrate that by doping the tungsten carbide nanoparticles with Co significantly increases their cytotoxic effect [15]. Based on the increased toxicity observed, the studies continued with the toxicity tests of Co-doped tungsten carbide nanoparticles, characterized by different sizes and morphologies, on various cell lines.

Thus, the cytotoxicity of the WC-Co particles, which are $40 \text{ }\mu\text{m}$ in diameter and both spherical and cortical, was evaluated. The toxicity study was evaluated using two pulmonary cell lines. This study has, in contrast, noted that the toxicity of these particles has no correlation between cytotoxicity with diameter and specific morphology of these nanoparticles [16]. Another study examined the WC-Co particle toxicity with particle size using lung epithelial cells. Thus, nanoparticles (98 nm) and WC-Co microparticles ($3.4 \text{ }\mu\text{m}$) have been shown to influence the toxicity in a dose-dependent and exposure time manner. Thus, nano-WC-Co particles have caused significant toxicity compared to micro-WC-Co

particles at lower concentrations and shorter exposure times. For the viability test, the cells were exposed to either nano- or microparticles at concentrations up to 1000 $\mu\text{g/mL}$ for exposure periods of time up to 48 hours. It has been observed that WC-Co nanoparticles have been internalized by the pulmonary epithelial cells, suggesting that internalization can play a key role in the increased toxicity of nanoparticles [17].

Furthermore, following all organs at risk in case of inhalation (lungs, liver, and kidneys), the cytotoxicity of WC-Co nanoparticles with a diameter of 60 nm was studied. In this study, the maximum concentration of nanoparticles added in cell medium was 150 $\mu\text{g/mL}$. These nanoparticles induce cellular mortality, DNA breaks in renal and hepatic cell lines, but do not induce significant cytotoxic effects in lung cells [18]. Based on these studies, WC-Co has been recognized by the National Institute for Occupational Safety and Health as presenting a health hazard to people after inhalation at the workplace. The use of these particles in the industrial field is high, and human health risks remain poorly studied, despite the fact that the International Agency for Research on Cancer (IARC) classifies them as “probably carcinogenic” materials for humans [18].

Beside the tungsten carbide, which was declared toxic in most of these studies, other tungsten alloys were considered relatively inert, and therefore some of these materials did not seem to present a significant risk for human toxicity. However, recent research findings have raised concerns about the possible adverse health effects after acute and chronic exposure to tungsten oxide. Based on unique biophysical properties, this material is considered an important candidate for a broad range of applications, starting with industrial use, with products such as flame-retardant fabrics, X-ray screens, gas sensors, automotive glass, or use as a pigment in ceramics and paints [19–22]. This material also finds application in the biomedical field [23] in the form of biological products like pigments, additives, and analytical agents [24]. Moreover, WO_3 nanoparticles are efficiently used as a contrast agent for computed tomography imaging [24].

Therefore, the toxicity of this material at a nanoscale dimension has begun to be carefully evaluated. It has been reported that these compounds of tungsten were absorbed after oral exposure in both man and rat organisms. Tungsten alloys incorporated into the body have been shown to cause metastatic tumors in rats. Tungsten oxide has been found to accumulate in several organs and/or tissues (kidneys, liver, ovaries, prostate, pancreas, lung, heart, muscles, spleen, and bones) after a single oral dose [25, 26]. Furthermore, at a nanometric scale, recent findings have shown that tungsten oxide nanoparticles have cytotoxic potential [23]. Various in vitro studies have shown that tungsten oxide, at higher concentrations, significantly increases the primary viability hepatocytes of rats [26] (0.3, 0.5 and 1 mg/mL). At the same time, even when a study highlighted nanotoxicity comparison between several materials, acute toxicity was observed in tungsten oxide at concentrations above 0.05–1 mg/mL [4].

Another study regarding tungsten oxide found it has cytotoxic effect on human alveolar epithelial cells, human epithelial colorectal cells, and murine fibroblast cell line at concentrations above 100 $\mu\text{g/mL}$ [11]. Contrary to these, the tungsten oxide nanoparticles are not toxic to these cells at low concentrations (3–100 $\mu\text{g/mL}$) and to human lung carcinoma (A549) cells [24]. In this article [18], a comparative study between tungsten oxide nanoparticles and microparticles was carried out. It was revealed that WO_3 nanoparticles induced a significant cell viability reduction and, at nanoscale dimension, increased cell membrane damage at higher doses (200 and 300 $\mu\text{g/mL}$, respectively). These results are in contrast with WO_3 microparticles. WO_3 microparticles did not incite any toxicity attributes in comparison to control samples for the tested concentrations.

1.3 Content of the chapter

After the short review regarding tungsten nanoparticles and the studies that were carried out until now regarding this particular toxicology, it resulted that the knowledge related to the toxicity of tungsten containing particles with tens and hundreds of nanometer size is limited or even missing. This dimension is particularly important because of low efficiency of particle collection by filters at this size scale. Moreover, we did not find any study that reveals the toxicity of tungsten nanoparticles on epithelial cells, despite the prevalence of the absorption of this material through the skin. Taking into account the possible release of tungsten nanoparticles into the atmosphere following a nuclear accident (LOVA) [12], nanoparticles would interact primarily with the epithelial tissue of the workers. This investigation is the further purpose of the present paper; and this is the reason why the normal human skin fibroblast cell line BJ ATCC CRL 2522 was chosen for toxicity evaluation after interaction with tungsten nanoparticles.

In order to undertake the cytotoxicity studies, tungsten dust has been purposely produced using the magnetron sputtering combined with gas aggregation (MS-GAS) technique. Scanning electron microscopy (SEM) and dynamic light scattering (DLS) were used to investigate the nanoparticle morphology and nanoparticle behavior in liquid medium, respectively. This synthesis method and also nanoparticles characterization will be presented in Section 2. In Section 3 toxicology studies will be presented. Doses with different concentrations of tungsten nanoparticles were used. At low concentration of tungsten nanoparticles, the cell viability was investigated using a cell viability assay MTS test ((3-(4, 5-dimethylthiazol-2-yl)-5-(3-carboxymethoxyphenyl)-2-(4-sulfophenyl)-2H-tetrazolium)). In contrast, at a higher concentration of tungsten particles, SEM was used to offer insights into the process of interactions between inorganic nanoparticles and epithelial cells. Also, for every nanoparticle concentration added over the skin cell culture, optical microscopy investigation was accomplished. Finally, in the Conclusions section, we elucidate if tungsten nanoparticles, characterized by a spherical shape and approximately 100 nm in diameter, present high toxicity or not with respect to human skin cells.

2. Nanoparticles synthesis and characterization

2.1 Synthesis of tungsten nanoparticles

Nanoparticles are generally synthesized using different methods largely presented in literature. These are classified mainly in chemical and physical ones [27–29]. In this work we preferred to use a physical synthesis method [30, 31]. Similar with the tokamak device, we have chosen a plasma-based method: magnetron sputtering combined with gas aggregation (MSGAG). This method was introduced in the last decade of the last century [32], and starting with that moment, it was used for the synthesis of nanoparticles based on different materials (which includes metals [33] and their compounds [34]).

The schematic figure of the experimental setup is presented in **Figure 1**. The setup assembled from two chambers, an aggregation chamber (MSGAG cluster source) which is attached to a vacuum deposition chamber. The cluster source consists in a water-cooled stainless-steel tube in which a magnetron sputtering plasma gun is mounted. The opposite face of the cluster source ends in a conical-shaped flange presenting a 1.5-mm aperture. The distance between the magnetron target (tungsten, 2" in diameter, purity of 99.95%) and the exit aperture defines the space

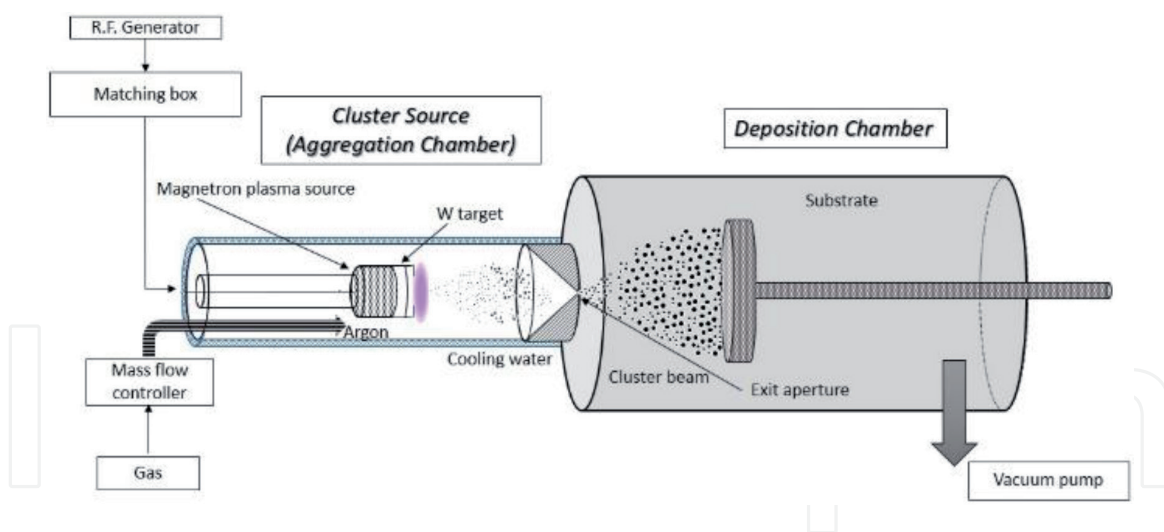


Figure 1.
Schematic of the experimental setup used for synthesis of tungsten nanoparticles.

where the aggregation of nanoparticles takes place; in this work the length of this space was 90 mm.

The following subsystems are integrated into the experimental system: a pumping unit consisting of a turbomolecular pump providing a high vacuum in both chambers and also pressure sensors; and the second subsystem is represented by the gas intake and the mass flow controller (MFC), which helps us control the gas flow in the chambers. In addition, in order to sustain the plasma discharge, a radio-frequency generator, provided with an impedance matching box, was used. The frequency used was 13.56 MHz, and the RF discharge power was constantly 80 W.

The process gas (Ar, 99.9999% purity) is fed directly in the aggregation chamber at a flow of 5 standard cubic centimeter per minutes (sccm), and it is evacuated (via the small aperture) by the pumping system of the deposition chamber. In MSGA system the working gas plays the following roles:

- i. To maintain the magnetron plasma discharge and thus, to produce by sputtering the tungsten atoms for nanoparticles growth.
- ii. To produce, by three body collisions ($W + W + Ar$), the initial germs (dimers of W-W type) for further growth of the nanoparticles.
- iii. To transport the nanoparticles from the cluster source in the deposition chamber via the exit aperture of the cluster source; this last action is sustained by the difference of pressure appearing between the deposition chamber (0.5 Pa) and the cluster source chamber (80 Pa).

In accord with the models for nanoparticles growth in magnetron sputtering plasmas presented in the literature [35], the W nanoparticles are formed in the following manner.

Firstly, the three body collisions taking place between two W atoms and an Ar one lead to the formation of W-W dimers. These act like initial germs and increase by further condensation of metallic vapors (process named accretion), until small nanocrystallites are formed. These present dimensions in between 2 and 10 nm. It is important to note that they may be charged; the charging proceeds by the interaction of nanocrystallites with plasma electrons (leading to negative charge) and ions (leading to positive charge). The electrostatic interaction gathers the nanocrystallites leading to formation of nanoparticles. This process is named coagulation.

Finally, the W nanoparticles are transported by the Ar flow in the deposition chamber, which are collected on glass and Si substrates (**Figure 2**). The deposition rate of WNP's was about 5 mg/hour.

2.2 Nanoparticles characterization

Before performing biological tests in order to evaluate the possible toxicity of tungsten nanostructures, aspects of nanoparticle morphology were investigated using SEM after which nanoparticle behavior in liquid medium was evaluated using DLS.

2.2.1 Morphological analysis by SEM

The laboratory model used to evaluate the possible toxic effect of tungsten dust was formed by a powder assembled from nanoparticles. This powder was extracted from the glass substrate and transferred on a carbon tape. The morphology of nanoparticles was investigated by SEM using a Zeiss EVO 50XVP with LaB₆ electron gun operating at 20 kV. **Figure 3** shows that the particles present almost spherical morphology. The diameter of the nanoparticles is about 100 nm.

2.2.2 Particle dispersion analysis by DLS

Nanoparticle behavior in liquid has to be studied as well, because the interaction with cells takes place in liquid phase. For the biological tests, liquid

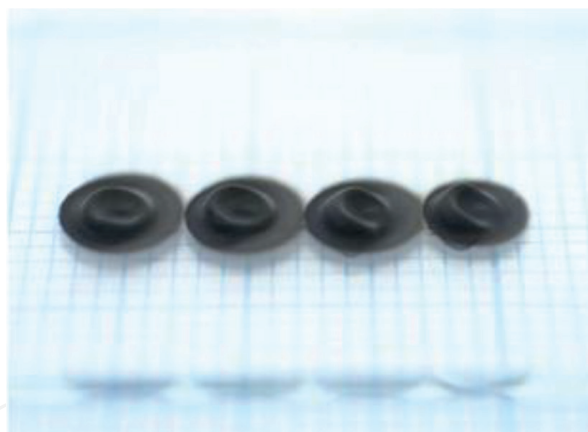


Figure 2.
Tungsten nanoparticle deposits, obtained after four different deposition runs, collected on glass substrate.

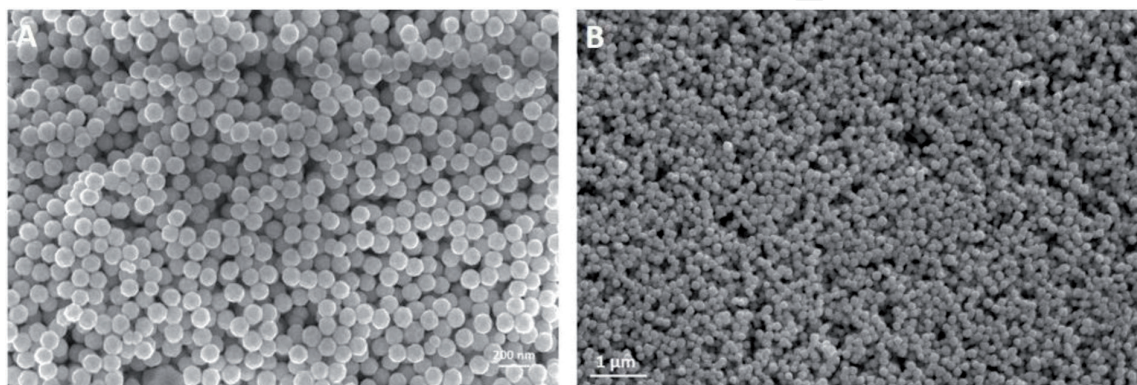


Figure 3.
SEM images of tungsten nanoparticle synthesized by MSGA technique: (A) higher magnification and (B) lower magnification.

dispersions of particles with various concentrations were prepared, as will be detailed in the next section. Such dispersions, consisting of particles dispersed in phosphate-buffered saline (PBS) solutions, were characterized by dynamic light scattering.

Dynamic light scattering (sometimes referred to as photon correlation spectroscopy or quasi-elastic light scattering) is a technique for measuring the size of particles dispersed in liquids, typically in the submicron scale. Dynamic light scattering actually determines the diffusion rate of particles in a particular dispersion medium as a result of the Brownian motion. Brownian motion is the random movement of particles due to the bombardment by the solvent molecules that surround them. Based on this physical process, this light scattering technique allows us to evaluate the apparent size that the particles reach when they are added in a liquid medium. The particles are illuminated with a laser beam with a power of 30 mW, and this light is scattered on the particles. The scattered light is then collected at an angle of 165° for size measurements and then measured with an extremely sensitive detector. After the detection, the hydrodynamic diameter is evaluated, which represents the diameter of a sphere having the same diffusion coefficient as the particle measured, also taking into account the layer of hydrates surrounding the particle/molecule [36].

The data analysis was performed with the DelsaNano 2.21 software. The results, obtained for three dispersion concentrations, used later in the biological tests, are presented in **Figure 4**.

It can be observed that the apparent diameter of nanoparticles in liquid is larger than the particle size indicated by SEM. Also the diameter increases with the concentration of nanoparticles added in liquid, indicating a tendency to agglomeration. The use of an ultrasonication procedure reduces the agglomeration, decreasing the apparent diameter.

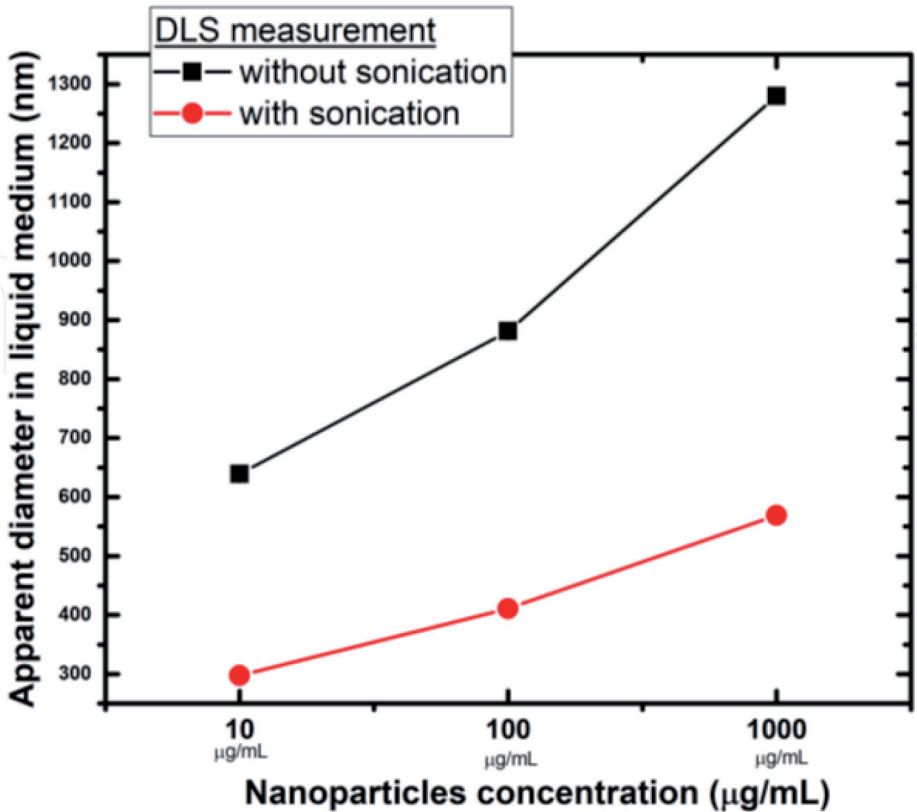


Figure 4. Apparent diameters resulted from DLS measurements at various dispersion concentrations (the concentrations of 10, 100, and 1000 µg/mL correspond to the samples indexed as C2, C3, and C4 in the Section 3).

3. Evaluation of toxicity

3.1 Cell line selection and preparation of cells samples

For the run of the biological assays, a human skin fibroblast culture, called BJ ATCC, CRL 2522, was used. These cells were derived from an initial ATCC lot (American Type Culture Collection) and were obtained from *Homo sapiens* species. This cell line was kept at 37°C in humidified atmosphere (5% CO₂). Fibroblasts were grown in the Eagle's minimum essential medium (EMEM) environment supplemented with 10% fetal bovine serum (FBS), 100 µg/mL penicillin and 100 µg/mL streptomycin (Figures 5 and 6).

3.2 Preparation of the biological samples

A working protocol was set to go from the nanoparticle synthesis (the nanoparticles gathered in circles in Figure 2) to the dilutions required to assess the toxicity. In order to achieve this goal, after synthesis, the nanoparticles were first collected from the substrate, weighed, and added in saline solution, forming a stock solution. Before being added over the inoculated cells, the stock solution was sterilized. Furthermore, dilutions were prepared from the stock, which were utilized for toxicity investigations. This protocol is described in Table 1 and illustrated in Figure 7.

In general, a decisive factor in the field of toxicology is determined by daily exposure to nanoparticles and the problem that arises due to it is that in vitro assays cannot be directly correlated with repeated exposure. Therefore, in the present study, in addition to the usual concentrations used for this type of analysis (1, 10, 100 µg/mL), two higher concentrations of nanoparticles were added in EMEM, concentrations that presents a major importance in the case of a nuclear accident, taking into account the purpose of the work [37]. In conclusion, dilutions from the stock suspension were made in order to obtain final concentrations of 1, 10, 100, 1000, and 2000 µg/mL, concentration used to evaluate the possible toxicity effect of tungsten nanoparticles (Table 2).

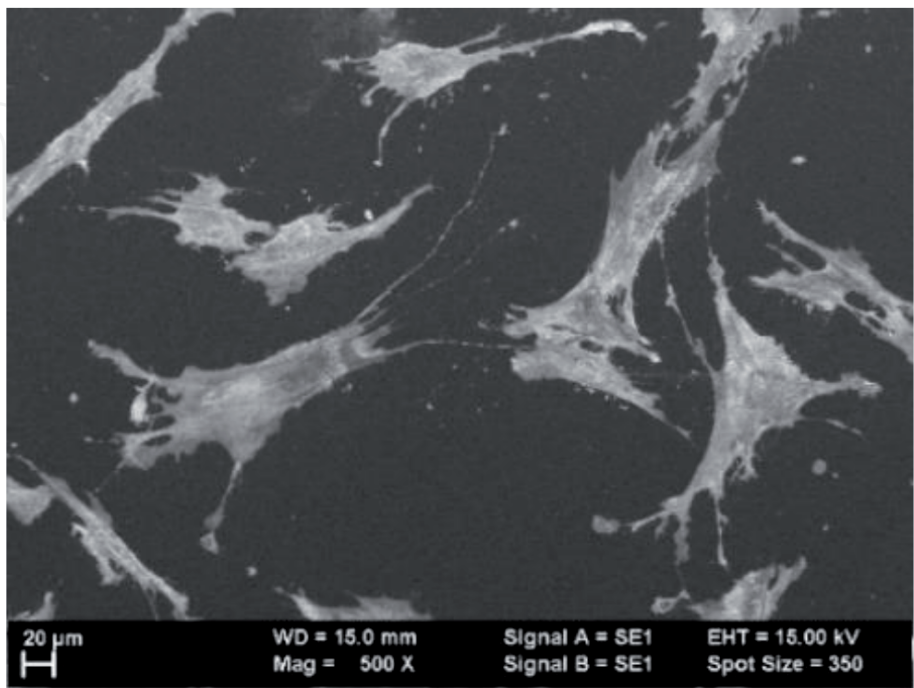


Figure 5.
SEM images of the fibroblast cells after being inoculated for 24 hours.

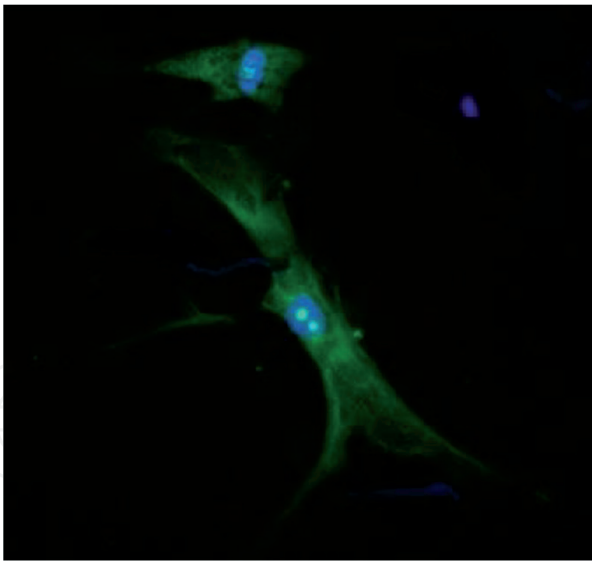


Figure 6.
Cells observed using a fluorescence microscope. Both the nucleus and the cell body are presented.

Preparation of nanoparticle samples to assess cytotoxicity	
Nanoparticles synthesis and collection on substrate	Step 1, Figure 2
Sampling nanoparticles from the glass substrates	Step 2, Figure 7
Weighing nanoparticle powders	Step 3, Figure 7
Preparation of the stock solution (10 mg/mL)	Step 4, Figure 7
Solution sterilization	Step 5, Figure 7
Performing dilutions, starting from the stock solution	Step 6, Figure 7

Table 1.
The steps required to prepare the samples for cytotoxicity evaluation.

At the same time when performing the particle dilutions, the cells were inoculated in the well plate. After the cell attachment on the bottom of the wells, in every well, a different dilution (from C1 up to C5) was added over the cells. This was the first step required to check on the interaction between nanoparticles and skin fibroblast cells, and in the following the meaning of the sample names is control sample for the sample with cells without nanoparticles; blanc for the sample with nanoparticles without cells; and C1, C2, C3, and C4 for the samples containing both cells and nanoparticles.

3.3 Optical microscopy investigation of interaction of cells with nanoparticle dilutions

For a first qualitative analysis of the influence of tungsten particles on dermal fibroblast cells, optical microscopy was used. The evaluation, after each step such as cell seeding in the wells, adding nanoparticle dispersions over the cells inoculated and analyzing beforehand cell viability with the MTS test, respectively, was carried out using the optical microscope inverted Olympus CKX31SF with 10×, 20×, and 40× magnifications.

At low concentrations (C2, C3), the cell attachment to the substrate is still present and the nanoparticle clusters are not well highlighted. We can conclude that cells are still viable in tungsten nanoparticle dispersion.

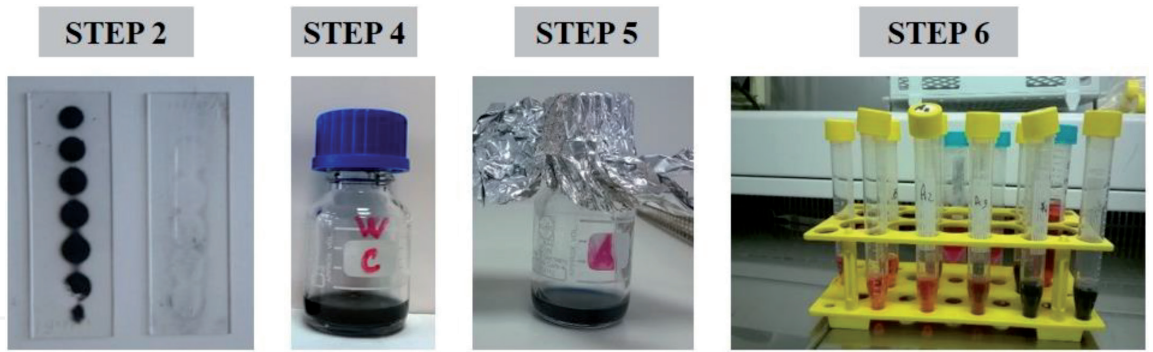


Figure 7. Images which illustrate the steps that were required for the preparation of nanoparticle samples to assess cytotoxicity.

C1	Low concentration of nanoparticles	1 µg/mL
C2		10 µg/mL
C3		100 µg/mL
C4	Higher concentration of nanoparticles	1000 µg/mL
C5		2000 µg/mL

Table 2. Dilutions based on stock concentration.

However, for higher concentrations, cells tend to be completely coated with nanoparticles, and moreover, it can be observed how certain cells change their shape, becoming round (a precursor for cell death), but we cannot be sure if the cells are still viable or not.

From the optical microscope images, it is possible to highlight that cells remain anchored on the substrate, even when the concentration of nanoparticles added to the medium is very high. This is an indication for cell viability and a suggestion that, at least in low concentration (<100 µg/mL), tungsten is certainly not a toxic material (**Figure 8**).

3.4 MTS test ((3-(4, 5-dimethylthiazol-2-yl)-5-(3-carboxymethoxyphenyl)-2-(4-sulfophenyl)-2H-tetrazolium))

The MTS ((3-(4,5-dimethylthiazol-2-yl)-5-(3-carboxymethoxyphenyl)-2-(4-sulfophenyl)-2H-tetrazolium)) test is a colorimetric method used for cytotoxicity analysis [38]. This test is used to quantify viable cells. This method is based on the mitochondrial oxidoreductase enzyme reduction by a tetrazolium salt (MTS compound). These enzymes are found only in viable cells—**Figure 9**. Thus, based on this interaction, a formazan compound is generated, and this compound is soluble in the culture environment. The presence of this compound changes the solution absorbance. The presence of the formazan compound is an index of mitochondrial activity, being proportional to the number of viable cells. Formazan exhibits maximum absorbance at 490 nm in a saline solution. Since the MTS reagent is sensitive to light, the test is performed by limiting the ambient light exposure. In addition, at higher concentration, the tungsten nanoparticles also change the dispersion absorbance, and this change interferes with formazan absorption. Therefore, the MTS test does not offer concluding results at high particle concentration, and this is the reason why we performed MTS investigation only for low-concentration samples

(C1, C2, and C3). Another method to evaluate the toxicity for high concentration of nanoparticles is required, and we conclude on this aspect using SEM investigations in Section 3.5.

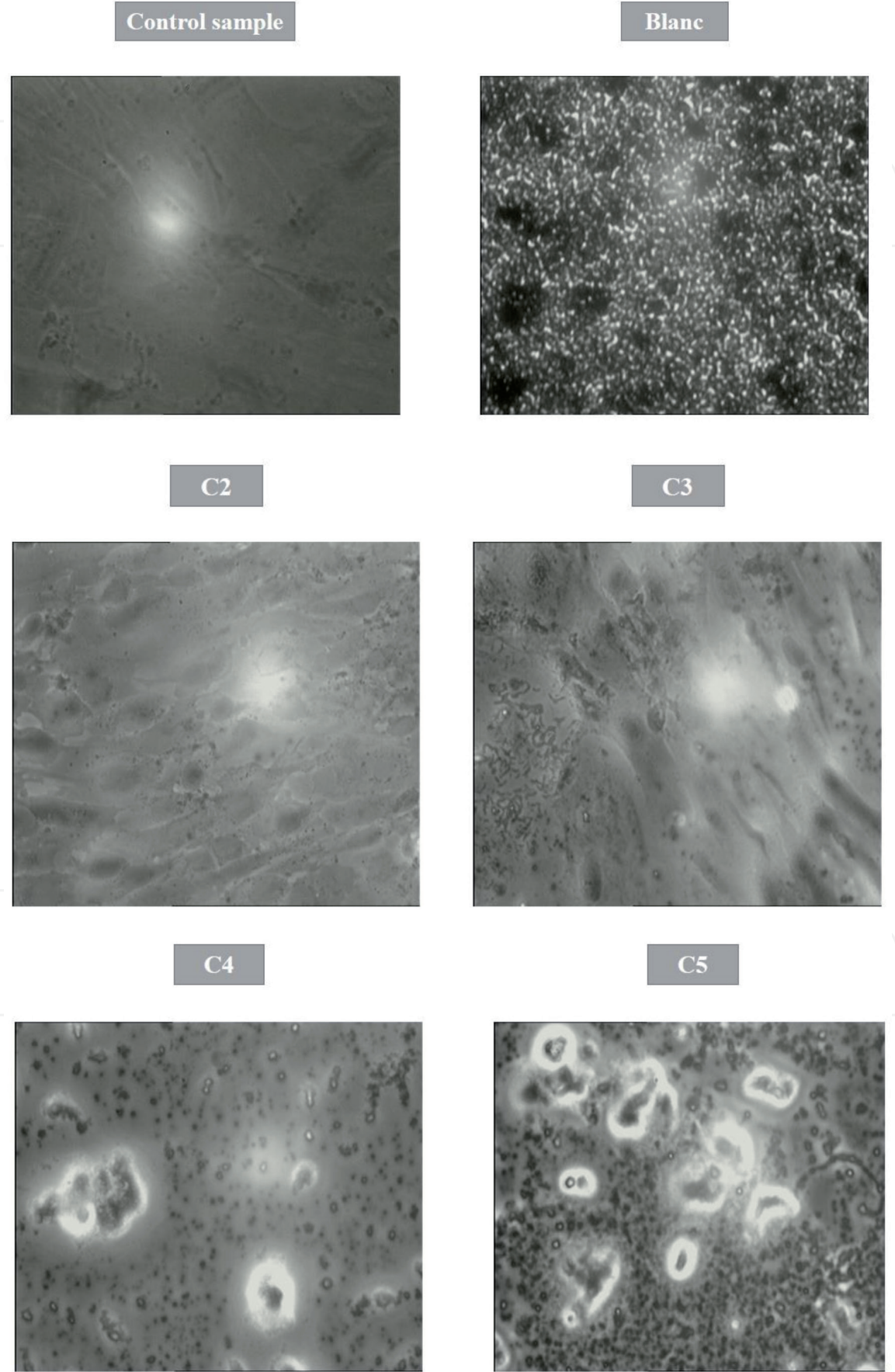


Figure 8.
Optical images of nanoparticle dispersions over the cells inoculated.

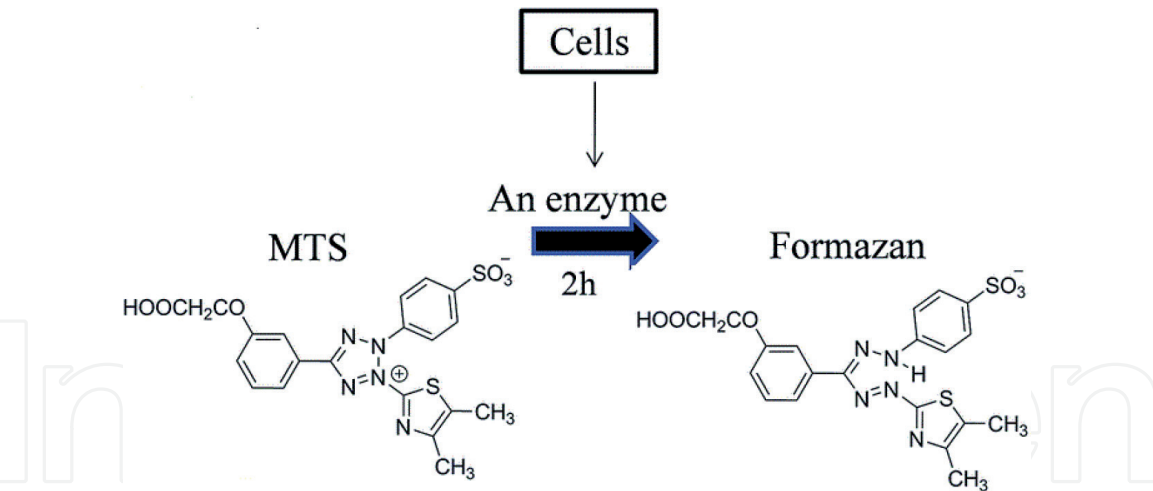


Figure 9.
The chemical structures of the MTS (((3-(4,5-dimethylthiazol-2-yl)-5-(3-carboxymethoxyphenyl)-2-(4-sulfophenyl)-2H-tetrazolium))) reagent and the formazan format compound obtained after the interaction between these compounds with the mitochondrial enzyme.

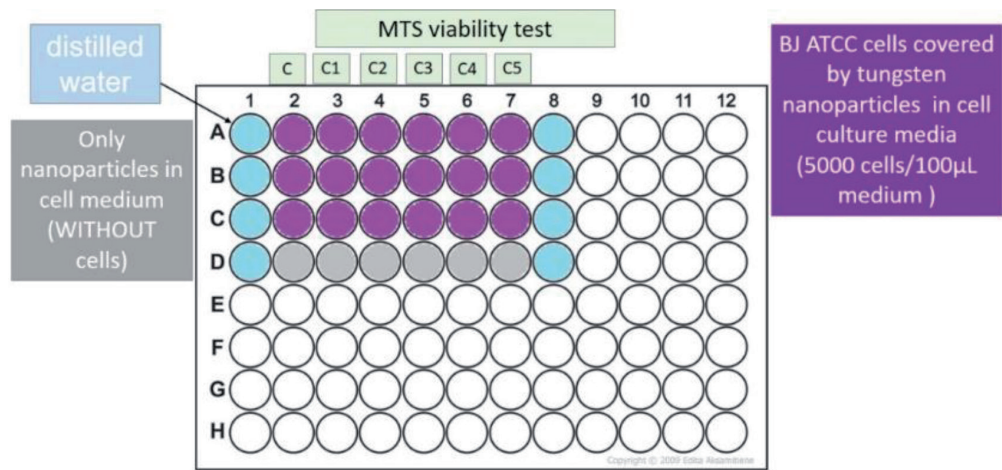


Figure 10.
Wells plate used for the evaluation of MTS assay. In this figure the use of every wells from the plate is highlighted.

Firstly, **Figure 10** shows the order in which different concentrations of tungsten were added over the inoculated cells in the well plates. **Figure 11** shows the MTS effect. MTS was added over dilutions before the cytotoxicity analysis. After 24 and 48 hours, respectively, nanoparticle suspensions were added over the cells inoculated in well plates, and MTS substance was pipetted into each well. This substance was left to act for 3 hours. The 96-well plate, as previously described, was introduced into Mithras spectrophotometer, Berthold Technologies, with the added MTS substance, for each well resulting in an absorbance value.

From the arithmetic average value of the three replicates, corresponding to each concentration (C1–C3), after the absorbance of the blanks was subtracted, the absorbance value was calculated using formula (1). The value of the viability percentage was calculated according to the control sample value, whose viability was considered 100%.

$$\text{Cell viability (C1 up to C3)} = \frac{\text{Absorbance value (C1 up to C3)} * 100}{\text{Control sample absorbance value}} \quad (1)$$

The MTS results, for 24 and 48 hours of interaction, are presented in **Figure 12**. The cytotoxic effect of WNP on cells is strongly influenced by the dilution

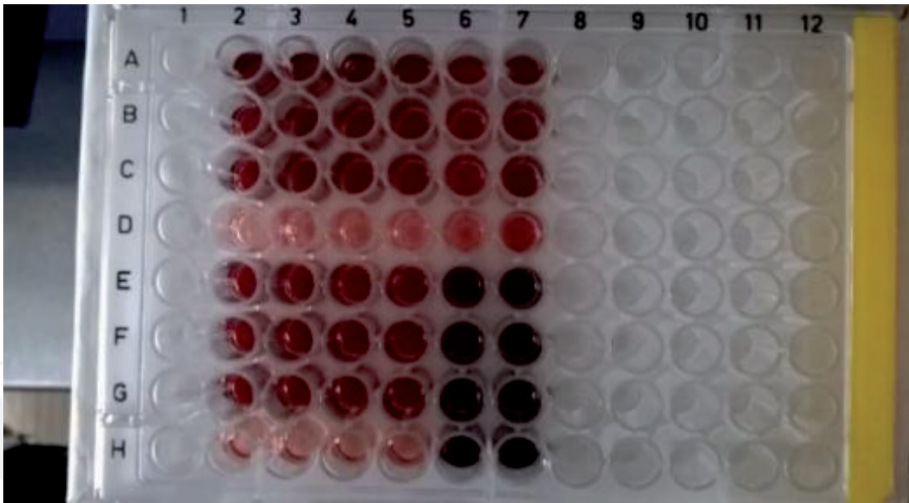


Figure 11.
The 96-well plate in which the MTS solution was put over the cells that were incubated for 24 hours. The formazan presence can be observed in wells by the change of the dispersion color.

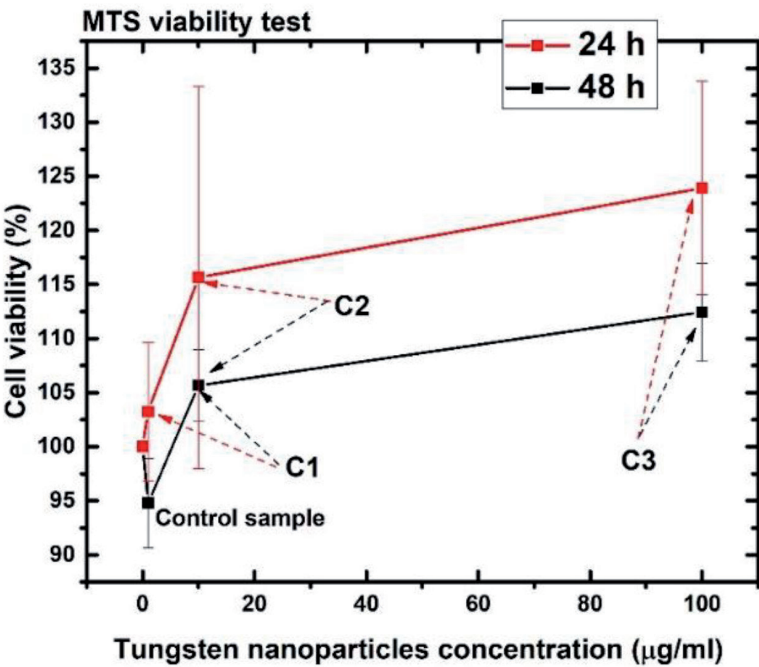


Figure 12.
Results of the MTS cell sample test after 24 and 48 hours, respectively, after the addition of nanoparticles over the anchored cells on the well. It can be seen how the viability decreases after 48 hours.

concentration. According to the results, at low concentrations, the tungsten nanoparticles are not toxic for human skin cells. Nevertheless, cell viability declines after 48 hours in comparison to 24 hours, which indicate that tungsten is not a material that helps cell proliferation.

3.5 Scanning electron microscopy investigations

Scanning electron microscopy was used to obtain complementary information on the process of interaction between the epithelial cells and nanoparticles. In this section, firstly, we will investigate the normal behavior of the cell attachment and cells morphology, in the absence of nanoparticles. In contrary, when different concentrations of nanoparticles were added over the cell culture (from C1 to C5), SEM examination informs us on the changes that can appear in their morphology and also in their viability. These aspects will be discovered using secondary electrons

(SE) imaging. In addition, by operating the instrument in the backscattered electron (BSE) imaging more, details from in-depth of the cell, like the presence of particles beyond the membrane thickness, can be revealed. This process, so-called internalization, is illustrated in **Figure 13**, where images of the same area cell,

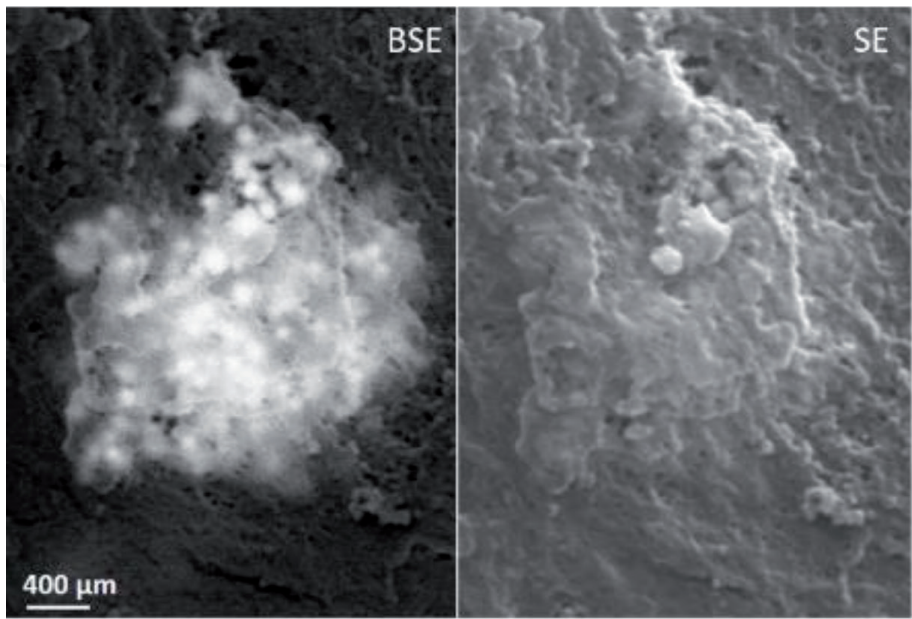


Figure 13.
SE and BSE images are compared and in the BSE image; the internalized particles are highlighted.

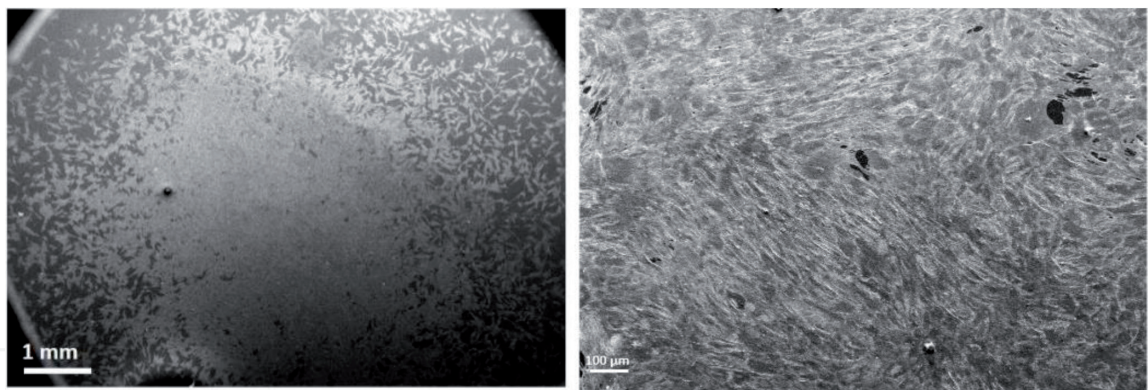


Figure 14.
SEM images, at low and higher magnification, of the control sample, taken using secondary electrons. Normal cellular development can be observed.

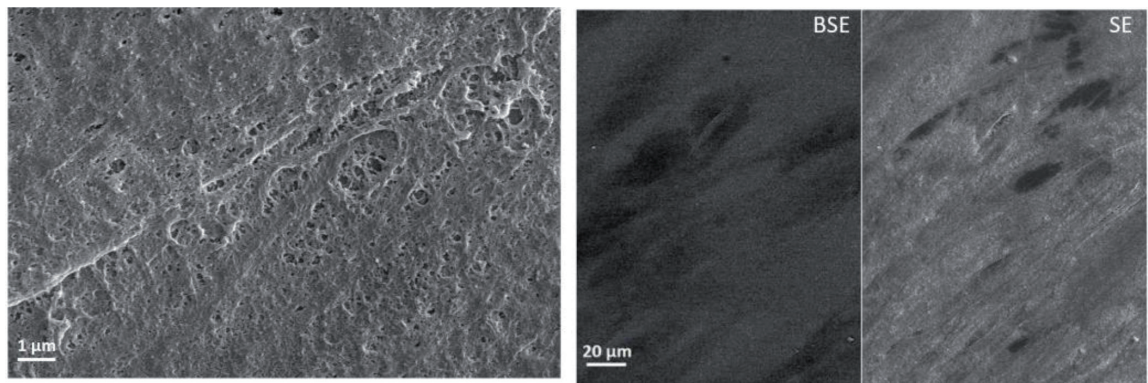


Figure 15.
SEM images taken with the secondary electron (SE) and backscattered electron (BSE) technique of a test sample, where no presence of nanoparticles is observed.

recorded in SE and BSE modes, are compared. Moreover, the backscattered electron technique is based on the contrast between different atomic numbers (Z), so that the nanoparticles with a higher atomic number (92) are brighter in these images than the cell body.

3.5.1 Control sample

In **Figure 14**, normal morphology of the fibroblast cell is observed for the control sample. It can be seen how cells tend to cover the entire surface of the well. An important point highlighted by the higher magnification image is the interconnection between cells. Using the backscattered electron technique (**Figure 15**, BSE compared to SE images), no sign of nanoparticles, or simply just impurity inside the cellular body, or any intrinsic cellular element that could affect the subsequent development of the cells can be observed.

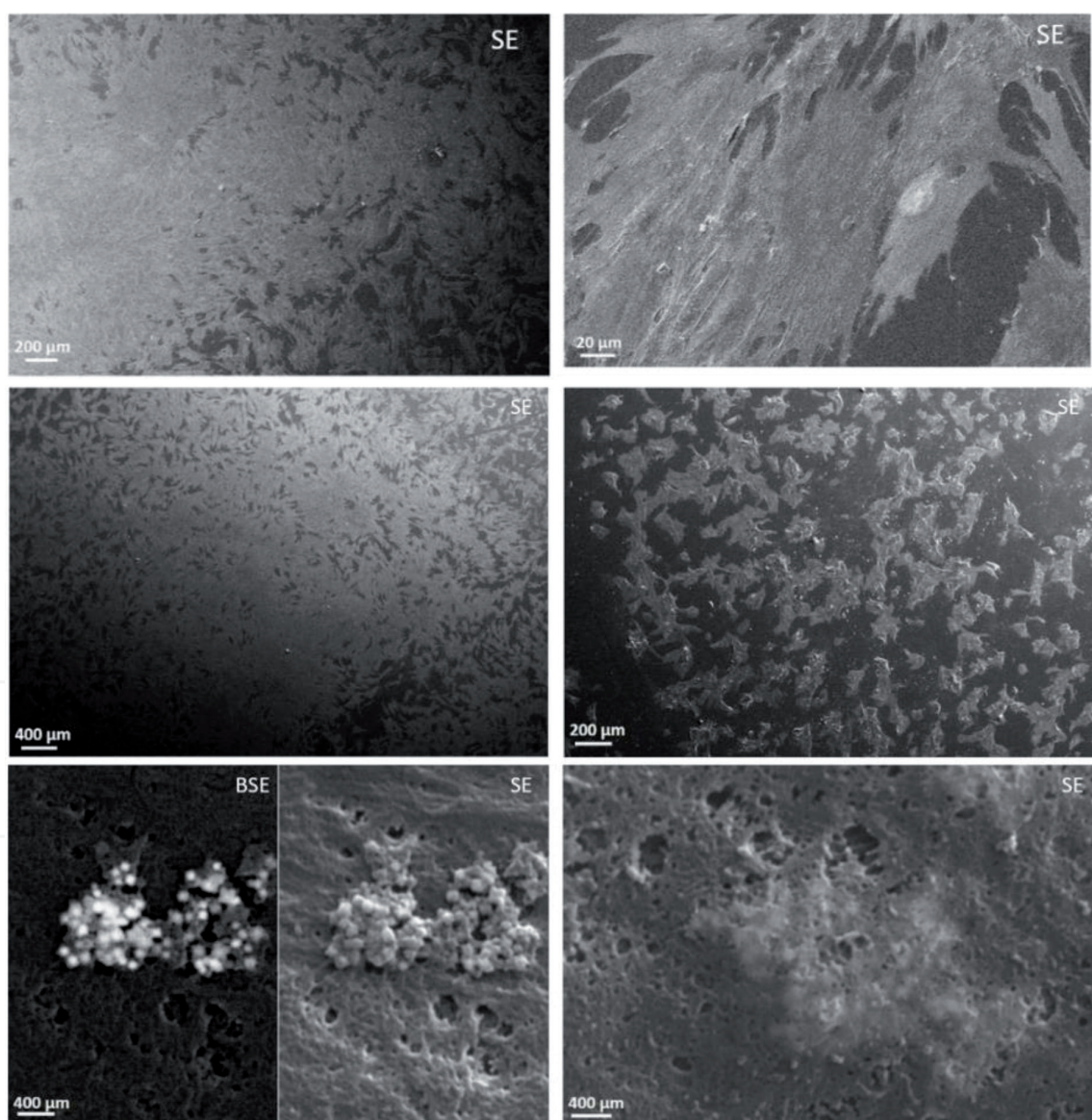


Figure 16.

Images of cells over which a small amount of tungsten nanoparticles (C1—1 $\mu\text{g/mL}$) were added. Even at such a small concentration added in the cellular environment, the presence of nanoparticles, both on the cell surface and inside the cell body, is observed. At the same time, a difference in the cell number and morphology can be observed in contrast with the control sample.

3.5.2 Low concentration of nanoparticles (samples C1 up to C3)

When a small amount of nanoparticles is added over the pre-inoculated cells, it can be observed first that the bonding between them is not destroyed and secondly, the nanoparticle presence does not radically modify cell morphology. However, some of them become slightly circular, and the number of attached cells on the well slightly decreases. Thus, at a low concentration, tungsten nanoparticles do not dramatically affect cellular proliferation, implicitly cellular viability, as it is demonstrated also by the MTS test. Nevertheless, a nanoparticle effect was observed. C1 nanoparticle concentration effects are present in **Figure 16**, while in **Figure 17** the C3 effects are highlighted.

3.5.3 Higher concentration of nanoparticles (C4 and C5)

At higher concentrations of nanoparticles added over the cells that were previously attached to the substrate, one can first notice a radical change in the cell morphology. They tend to become round, a sign that precedes cell death. At the same time, the number of cells attached on the walls decreased in contrast with the control sample, which shows that the nanoparticles obviously affect the proliferation of fibroblast cells, effects presented in **Figures 18** and **19** for

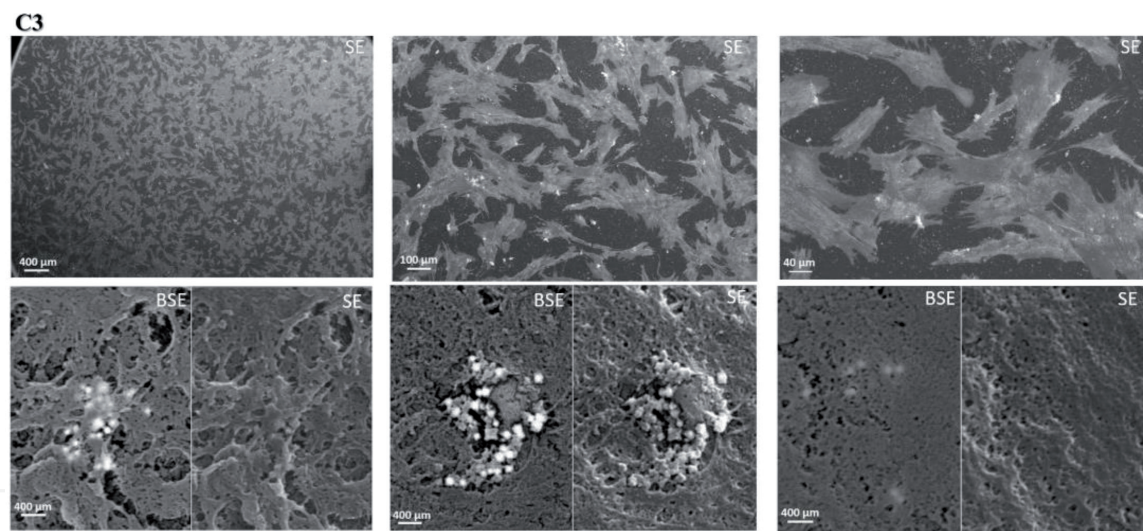


Figure 17. When the amount of nanoparticles added over attached cells increases (C3—100 µg/mL), a decrease in the cell number on the well surface can be seen, and the number of nanoparticles on the cell surface, as well as the number of nanoparticles internalized in the body of the cells, is higher.

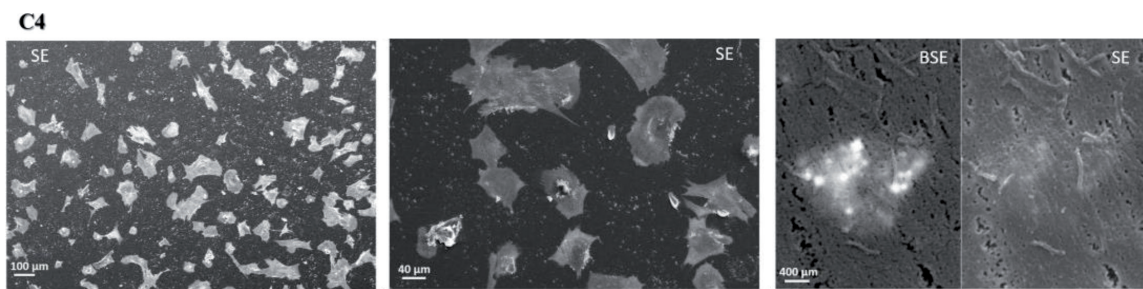


Figure 18. Images taken with the help of secondary electron (SE) and backscattered electron techniques (BSE) that highlight the changes in cell morphology after interaction with tungsten nanoparticles.

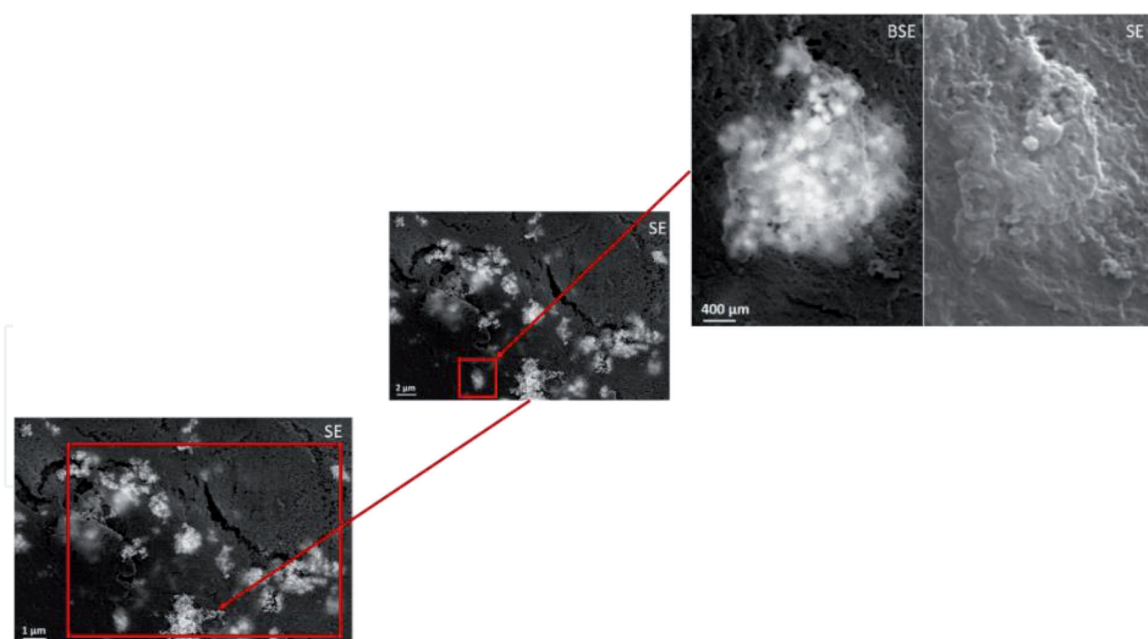


Figure 19.

Images taken with the help of secondary electron (SE) and backscattered electron techniques (BSE) at various magnifications that capture the effect of nanoparticles when large amounts of them were added over inoculated fibroblast cells.

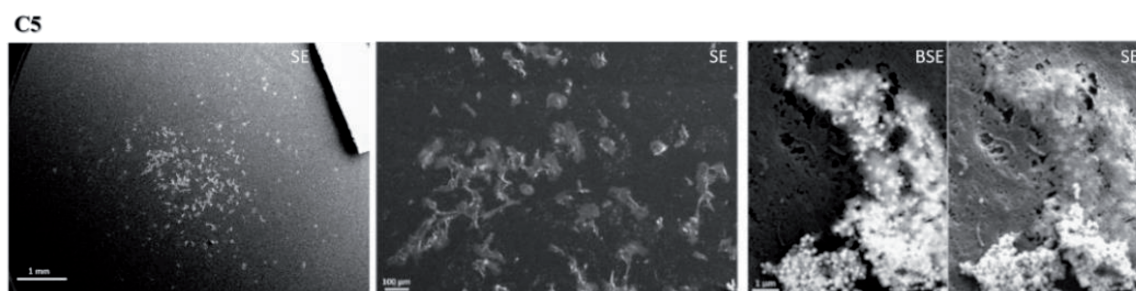


Figure 20.

Electron microscopy images at various magnifications that capture the effect of nanoparticles when a very high concentration of cellular media mixed with nanoparticles is added over the inoculated fibroblast cells. These nanoparticles influence the growth of cells because they remain on the surface, but at the same time, some of them also penetrate the cellular body, beneath the membrane.

C4 concentration and **Figures 20 and 21**, for C5 concentration, respectively. At a higher magnification, it is noticeable that the nanoparticles were internalized under the cell membrane, an effect that is highlighted using the backscattered electron technique.

This section shows that no major difference can be seen between the control sample, in which cells have grown normally and the sample of cells over which just a small amount of nanoparticles (e.g., sample C1) has been added. In contrast, when nanoparticle concentration increased, the number of viable cells attached on the well decreased, this being especially noticeable at a low magnification. However, when the magnification increases, it can be observed that nanoparticles cover approximately the entire cell surface, and moreover, they penetrate the membrane, being internalized in the cells (**Figure 21**). This could be observed with back-scattered electrons that nanoparticles can penetrate the cells at a depth of about 100 nm, meaning within the cytoplasm (under the membrane, this being defined by the lipid bilayer having the thickness about 10 nm).

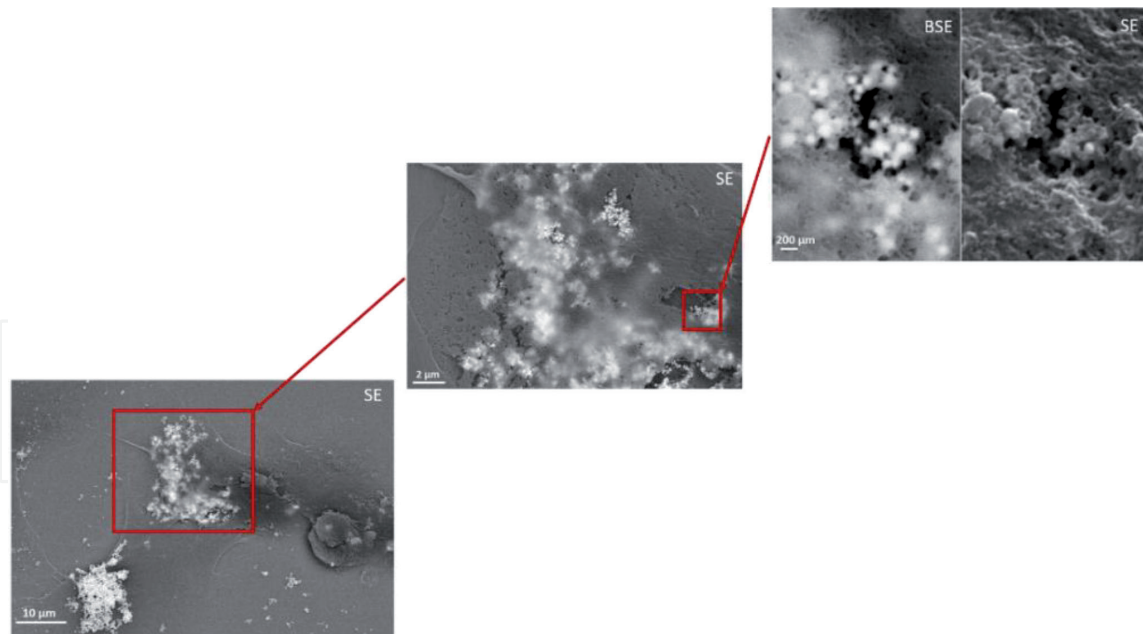


Figure 21.
 Images taken using scanning electron microscopy at various magnifications, observing C5 concentration of nanoparticles (2 mg/mL), both on the surface of the cell body and nanoparticles that are internalized under the membrane. These latter nanoparticles can be observed through the backscattered electron technique.

4. Conclusions

This chapter addresses a high-profile scientific field in which we evaluate the possible cytotoxic effects of tungsten nanoparticles through their in vitro exposure. Firstly, according to the chosen research theme, a laboratory model was used in order to investigate the possible toxicity of the tungsten dust. This laboratory model was used to simulate the nanoparticles resulting from a nuclear fusion reactor operation. This model is based on nanoparticle synthesis using the magnetron sputtering with the gas aggregation technique.

This chapter specifically focuses on assessing the toxicity of tungsten particles on fibroblast cells. The toxicity of tungsten powder in dispersion was tested using dermal fibroblast cells. For this investigation, different concentrations of nanoparticles added to the previously inoculated cells in the wells were used. Thus, at low concentrations of nanoparticles added in suspension, this material does not exhibit a high level of toxicity. However, when the nanoparticle concentration added to the cellular medium increases above 100 µg/mL, reaching even 1 and 2 mg/mL doses of interest in accordance with to the concentration of nanoparticles released following a possible nuclear accident (LOVA), the toxicity of tungsten is high. This toxicity is primarily observed by significantly reducing the number of viable cells remaining on the substrate. Thus, the ability to multiply in monolayer is lost due to the nanoparticle destruction of the contact between the neighboring cells. Furthermore, loss of cell contact with the surface of the well can be observed. Thus, individual cells appear on the surface. At the same time, optical investigation has observed the change in cell morphology. They tend to have a spherical shape, by retracting their pseudopods. These changes occurring in dermal fibroblast cells after interaction with tungsten nanoparticles are characteristic of the post-apoptotic stage.

Acknowledgements

Part of this work has been carried out within the framework of the Eurofusion consortium and has received funding from the Euratom research and training programme 2014–2018 and 2019–2020 (work package WPEDU-RO, ctr. 1EU-12) under grant agreement No 633053. The views and opinions expressed herein do not necessarily reflect those of the European Commission. In addition, we acknowledge the support in the frame of IFA-CEA project C5-07/2016 and Core Programme 2019 at INFLPR.

Conflict of interest

The authors declare that there is no conflict of interest.

Notes/thanks/other declarations

Author details

Lavinia Gabriela Carpen^{1,2}, Tomy Acsente¹, Maria Adriana Acasandrei³, Elena Matei⁴, Claudia Gabriela Chilom², Diana Iulia Savu³ and Gheorghe Dinescu^{1,2*}

1 National Institute for Laser, Plasma and Radiation Physics (INFLPR), Bucharest, Romania

2 Faculty of Physics, University of Bucharest, Bucharest, Romania

3 Horia Hulubei National Institute for R & D in Physics and Nuclear Engineering (IFIN-HH), Bucharest, Romania

4 National Institute of Materials Physics (NIMP), Bucharest, Romania

*Address all correspondence to: dinescug@infim.ro

IntechOpen

© 2019 The Author(s). Licensee IntechOpen. This chapter is distributed under the terms of the Creative Commons Attribution License (<http://creativecommons.org/licenses/by/3.0>), which permits unrestricted use, distribution, and reproduction in any medium, provided the original work is properly cited. 

References

- [1] Hussain SM, Hess KL, Gearhart JM, Geiss KT, Schlager JJ. In vitro toxicity of nanoparticles in BRL 3A rat liver cells. *Toxicology in Vitro*. 2005;**19**:975-983. DOI: 10.1016/j.tiv.2005.06.034
- [2] Khanna P, Ong C, Bay BH, Baeg GH. Nanotoxicity: An interplay of oxidative stress, inflammation and cell death. *Nanomaterials*. 2015;**5**:1163-1180. DOI: 10.3390/nano5031163
- [3] Zhao Y, Wang B, Feng W, Bai C. Nanotoxicology: Toxicological and biological activities of nanomaterials. In: *Encyclopedia of Life Support Systems (EOLSS)*. 2011. p. 26
- [4] Jain K, Kohli E, Prasad D, Kamal SSK, Haussain SM, Singh SB. In vitro cytotoxicity assessment of metal oxide nanoparticle. *Nanomedicine and Nanobiology*. 2014;**1**(1):10-19. DOI: 10.1166/nmb.2014.1003
- [5] Grabinski C, Hussain S, Lafdi K, Braydich-Stolle L, Schlager J. Effect of particle dimension on biocompatibility of carbon nanomaterials. *Carbon*. 2007;**45**(14):2828-2835. DOI: 10.1016/j.carbon.2007.08.039
- [6] Li X, Liu W, Sun L, Aifantis KE, Yu B, Fan Y, et al. Effects of physicochemical properties of nanomaterials on their toxicity. *Journal of Biomedical Materials Research*. 2015;**103**(7):2499-2507. DOI: 10.1002/jbm.a.35384
- [7] Proksch E, Brandner JM, Jensen JM. The skin: An indispensable barrier. *Experimental Dermatology*. 2008;**17**(12):1063-1072. DOI: 10.1111/j.1600-0625.2008.00786.x
- [8] Bennat C, Müller-Goymann CC. Skin penetration and stabilization of formulations containing microfine titanium dioxide as physical UV filter. *International Journal of Cosmetic Science*. 2000;**22**(4):271-283. DOI: 10.1046/j.1467-2494.2000.00009.x
- [9] Trop M, Novak M, Rodl S, Hellbom B, Kroell W, Goessler W. Silver-coated dressing acticoat caused raised liver enzymes and argyria-like symptoms in burn patient. *The Journal of Trauma Injury Infection and Critical Care*. 2006;**60**(3):648-658. DOI: 10.1097/01.ta.0000208126.22089.b6
- [10] Tinkle SS, Antonini JM, Rich BA, Roberts JR, Salmen R, DePree K, et al. Skin as a route of exposure and sensitization in chronic beryllium disease. *Environmental Health Perspectives*. 2003;**111**:1202-1208. DOI: 10.1289/ehp.5999
- [11] Ivask A, Titma T, Visnapuu M, Vija H, Kärkinen A, Sihtmäe M, et al. Toxicity of 11 metal oxide nanoparticles to three mammalian cell types in vitro. *Current Topics in Medicinal Chemistry*. 2015;**15**(18):1914-1929. DOI: 10.2174/1568026615666150506150109
- [12] Malizia A, Poggi LA, Ciparisse J-F, Rossi R, Bellecci C, Gaudi P. A: Review of dangerous dust in fusion reactors: From its creation to its resuspension in case of LOCA and LOVA. *Energies*. 2016;**9**:578. DOI: 10.3390/en9080578
- [13] Prajapati MV, Adebolu OO, Morrow BM, Cerreta JM. Evaluation of pulmonary response to inhaled tungsten (IV) oxide nanoparticles in golden Syrian hamster. *Experimental Biology and Medicine*. 2017;**242**:29-44. DOI: 10.1177/1535370216665173
- [14] Bolt AM, Sabourin V, Molina MF, Police AM, Negro Silva LF, Plourde D, et al. Tungsten targets the tumor microenvironment to enhance breast cancer metastasis. *Toxicological Sciences*. 2015;**143**(1):165-177. DOI: 10.1093/toxsci/kfu219

- [15] Bastian S, Busch W, Kühnel D, Springer A, Meißner T, Holke R, et al. Toxicity of tungsten carbide and cobalt doped tungsten carbide nanoparticles in mammalian cells in vitro. *Environmental Health Perspectives*. 2009;**117**(4):530-536. DOI: 10.1289/ehp.0800121
- [16] Lanone S, Rogerieux F, Geys J, Dupont A, Maillot-Marechal E, Boczkowski J, et al. Comparative toxicity of 24 manufactured nanoparticles in human alveolar epithelial and macrophage cell lines. *Particle and Fibre Toxicology*. 2009;**6**:12. DOI: 10.1186/1743-8977-6-14
- [17] Armstead AL, Arena CB, Li B. Exploring the potential role of tungsten carbide cobalt (WC-Co) nanoparticle internalization in observed toxicity toward lung epithelial cells in vitro. *Toxicology and Applied Pharmacology*. 2014;**278**(1):1-8. DOI: 10.1016/j.taap.2014.04.008
- [18] Paget V, Moche H, Kortulewski T, Grall R, Irbah L, Nessler F, et al. Human cell line-dependent WC-Co nanoparticle cytotoxicity and genotoxicity: A key role of ROS production. *Toxicological Sciences*. 2015;**143**(2):385-397. DOI: 10.1093/toxsci/kfu238
- [19] Lassner E, Schubert W-D. *Tungsten-Properties, Chemistry, Technology of the Element, Alloys, and Chemical Compounds*. 1st ed. New York, US: Springer; 1999. p. 422. DOI: 10.1007/978-1-4615-4907-9
- [20] Lee WJ, Fang YK, Ho J-J, Hsieh W-T, Ting S-F, Huang D, et al. Effects of surface porosity on tungsten trioxide (WO₃) films electrochromic performance. *Journal of Electronic Materials*. 2000;**29**(2):183-187. DOI: 10.1007/s11664-000-0139-8
- [21] Williams DE, Aliwell SR, Pratt KFE, Caruana DJ, Jones RL, Cox RA, et al. Modelling the response of a tungsten oxide semiconductor as a gas sensor for the measurement of ozone. *Measurement Science and Technology*. 2002;**13**(6):923-931. DOI: 10.1088/0957-0233/13/6/314
- [22] Patnaik P. *Handbook of Inorganic Chemicals*. 1st ed. McGraw-Hill Professional: USA; 2002. p. 1086
- [23] Akbaba BG, Turkez H, Sonmez E, Akbaba U, Aydın E, Tatar A, et al. In vitro genotoxicity evaluation of tungsten (VI) oxide nanopowder using human lymphocytes. *Biomedical Research*. 2016;**27**(1):229-234
- [24] Chinde S, Poornachandra Y, Panyala A, Kumari SI, Yerramsetty S, Adicherla H, et al. Comparative study of cyto- and genotoxic potential with mechanistic insights of tungsten oxide nano- and microparticles in lung carcinoma cells. *Journal of Applied Toxicology*. 2018;**38**:896-913. DOI: 10.1002/jat.3598
- [25] McInturf SM, Bekkedal MY, Wilfong E, Arfstend D, Gunasekar PG, Chapman GD. Neurobehavioral effects of sodium tungstate exposure on rats and their progeny. *Neurotoxicology and Teratology*. 2008;**30**(6):455-461. DOI: 10.1016/j.ntt.2008.07.003
- [26] Turkez H, Sonmez E, Turkez O, Mokhtar YI, Di Stefano A, Turgut G. The risk evaluation of tungsten oxide nanoparticles in cultured rat liver cells for its safe applications in nanotechnology. *Brazilian Archives of Biology and Technology*. 2014;**57**(4):532-541. DOI: 10.1590/S1516-89132014005000021
- [27] Lazea Stoyanova A, Vlad A, Vlaicu AM, Teodorescu VS, Dinescu G. Synthesis of copper particles by non-thermal atmospheric pressure plasma jet. *Plasma Processes and Polymers*. 2015;**12**(8). DOI: 10.1002/ppap.201400197

- [28] Lazea-Stoyanova A, Enculescu M, Vizireanu S, Marascu V, Dinescu G. Effects of process parameters on growth of metal particles by atmospheric pressure plasma jet. *Digest Journal of Nanomaterials and Biostructures*. 2014;**9**(3):1241-1247
- [29] Marascu V, Lazea-Stoyanova A, Stancu C, Dinescu G. The influence of plasma operation parameters on synthesis process of copper particles at atmospheric pressure. *Plasma Processes and Polymers*. 2018;**15**(1). DOI: 10.1002/ppap.201700091
- [30] Acsente T, Negrea RF, Nistor LC, Logofatu C, Matei E, Birjega R, et al. Synthesis of flower-like tungsten nanoparticles by magnetron sputtering combined with gas aggregation. *The European Physical Journal*. 2015;**69**(6):7. DOI: 10.1140/epjd/e2015-60097-4
- [31] Acsente T, Negrea RF, Nistor LC, Matei E, Grisolia C, Birjega R, et al. Tungsten nanoparticles with controlled shape and crystallinity obtained by magnetron sputtering and gas aggregation. *Materials Letters*. 2015;**200**:121-124. DOI: 10.1016/j.matlet.2017.04.105
- [32] Haberland H, Karrais M, Mall M, Thurner Y. Thin films from energetic cluster impact: A feasibility study. *Journal of Vacuum Science and Technology*. 1992;**A10**:3266. DOI: 10.1116/1.577853
- [33] Haberland H, Karrais M, Mall M. A new type of cluster and cluster ion source. *Zeitschrift fur Physik D: Atoms, Molecules and Clusters*. 1991;**20**(1):413-415. DOI: 10.1007/BF01544025
- [34] Shelemin A, Kylián O, Hanuš J, Choukourov A, Melnichuk I, Serov A, et al. Preparation of metal oxide nanoparticles by gas aggregation cluster source. *Vacuum*. 2015;**A120**:162-169. DOI: 10.1016/j.vacuum.2015.07.008
- [35] Kashtanov PV, Smirnov BM, Hippler R. Magnetron plasma and nanotechnology. *Physics-Uspekhi*. 2007;**50**(5):455-488. DOI: 10.1070/PU2007v050n05ABEH006138
- [36] Tantra R, Schulze P, Quincey P. Effect of nanoparticle concentration on zeta-potential measurement results and reproducibility. *Particuology*. 2010;**8**:279-285. DOI: 10.1016/j.partic.2010.01.003
- [37] Drasler B, Sayre P, Steinhäuser KG, Petri-Fink A, Rothen-Rutishauser B. In vitro approaches to assess the hazard of nanomaterials. *NanoImpact*. 2017;**8**:99-116. DOI: 10.1016/j.impact.2017.08.002
- [38] Cory AH, Owen TC, Barltrop JA, Cory JG. Use of an aqueous soluble tetrazolium/formazan assay for cell growth assays in culture. *Cancer Communications*. 1991;**3**(7):207-212. DOI: 10.1016/0022-1759(93)90092-L